ISSN 0006-2979, Biochemistry (Moscow), 2011, Vol. 76, No. 11, pp. 1233-1241. © Pleiades Publishing, Ltd., 2011.
Published in Biokhimiya, 2011, Vol. 76, No. 11, pp. 1532-1541.
Originally published in Biochemistry (Moscow) On-Line Papers in Press, as Manuscript BM11-171, September 11, 2011.

Contribution of Conserved Glu255 and Cys289 Residues to Catalytic Activity of Recombinant Aldehyde Dehydrogenase from *Bacillus licheniformis*

Yen-Chung Lee[1], Den-Tai Lin[1], Ping-Ling Ong[2], Hsiang-Ling Chen[3], Huei-Fen Lo[3]*, and Long-Liu Lin[4]*

[1]*Department of Bioagricultural Science, National Chiayi University, 300 Syuefu Road, Chiayi City 60004, Taiwan*
[2]*Department of Biochemical Science and Technology, National Chiayi University, 300 Syuefu Road, Chiayi City 60004, Taiwan*
[3]*Department of Food Science and Technology, Hungkuang University, Shalu, Taichung City, Taiwan; fax: +886(4)2631-9176; E-mail: hflo@sunrise.hk.edu.tw*
[4]*Department of Applied Chemistry, National Chiayi University, 300 Syuefu Road, Chiayi City 60004, Taiwan; fax: +886(0)5271-7901; E-mail: llin@mail.ncyu.edu.tw*

Received June 1, 2011
Revision received June 8, 2011

Abstract—Based on the sequence homology, we have modeled the three-dimensional structure of *Bacillus licheniformis* aldehyde dehydrogenase (*Bl*ALDH) and identified two different residues, Glu255 and Cys289, that might be responsible for the catalytic function of the enzyme. The role of these residues was further investigated by site-directed mutagenesis and biophysical analysis. The expressed parental and mutant proteins were purified by nickel-chelate chromatography, and their molecular masses were determined to be approximately 53 kDa by SDS-PAGE. As compared with the parental *Bl*ALDH, a dramatic decrease or even complete loss of the dehydrogenase activity was observed for the mutant enzymes. Structural analysis showed that the intrinsic fluorescence and circular dichroism spectra of the mutant proteins were similar to the parental enzyme, but most of the variants exhibited a different sensitivity towards thermal- and guanidine hydrochloride-induced denaturation. These observations indicate that residues Glu255 and Cys289 play an important role in the dehydrogenase activity of *Bl*ALDH, and the rigidity of the enzyme has been changed as a consequence of the mutations.

DOI: 10.1134/S0006297911110058

Key words: aldehyde dehydrogenase, *Bacillus licheniformis*, site-directed mutagenesis, dehydrogenase activity, fluorescence, circular dichroism

The extended family of aldehyde dehydrogenases (ALDHs) contains well over 150 different proteins composed of polypeptides approximately 50-55 kDa in molecular mass [1]. These enzymes are known to catalyze the irreversible $NAD(P)^+$-dependent oxidation of a wide variety of aliphatic and aromatic aldehydes to their corresponding acids. Aldehydes are cytotoxic and mutagenic compounds that are present in the environment as a result of industrial activity [2] and are formed endogenously during the metabolism of amino acids, vitamins, lipids, and carbohydrates [3]. Since the dehydrogenase activity plays an important role as the detoxifying agent to overcome the harmful effects of aldehydic compounds, the biochemical properties of a variety of eukaryotic, archaeal, and prokaryotic ALDHs has been determined [4-11]. Furthermore, the ALDH gene and protein families have been analyzed and updated [12-14]. Based on the sequences, the extended ALDH family can be divided into at least 13 different classes, some of which have quite specific and others broad substrate preferences.

Several crystal structures of the ALDH proteins have been determined, starting with *Rattus norvegicus* ALDH3 (*Rn*ALDH3) [15] and extending to *Bos taurus* ALDH2 (*Bt*ALDH2) [16], *Gadus callarias* ALDH9 (*Gc*ALDH9)

Abbreviations: AEW, average emission wavelength; ALDH, aldehyde dehydrogenase; IPTG, isopropyl β-D-thiogalactopyranoside; LB, Luria–Bertani medium.

* To whom correspondence should be addressed.

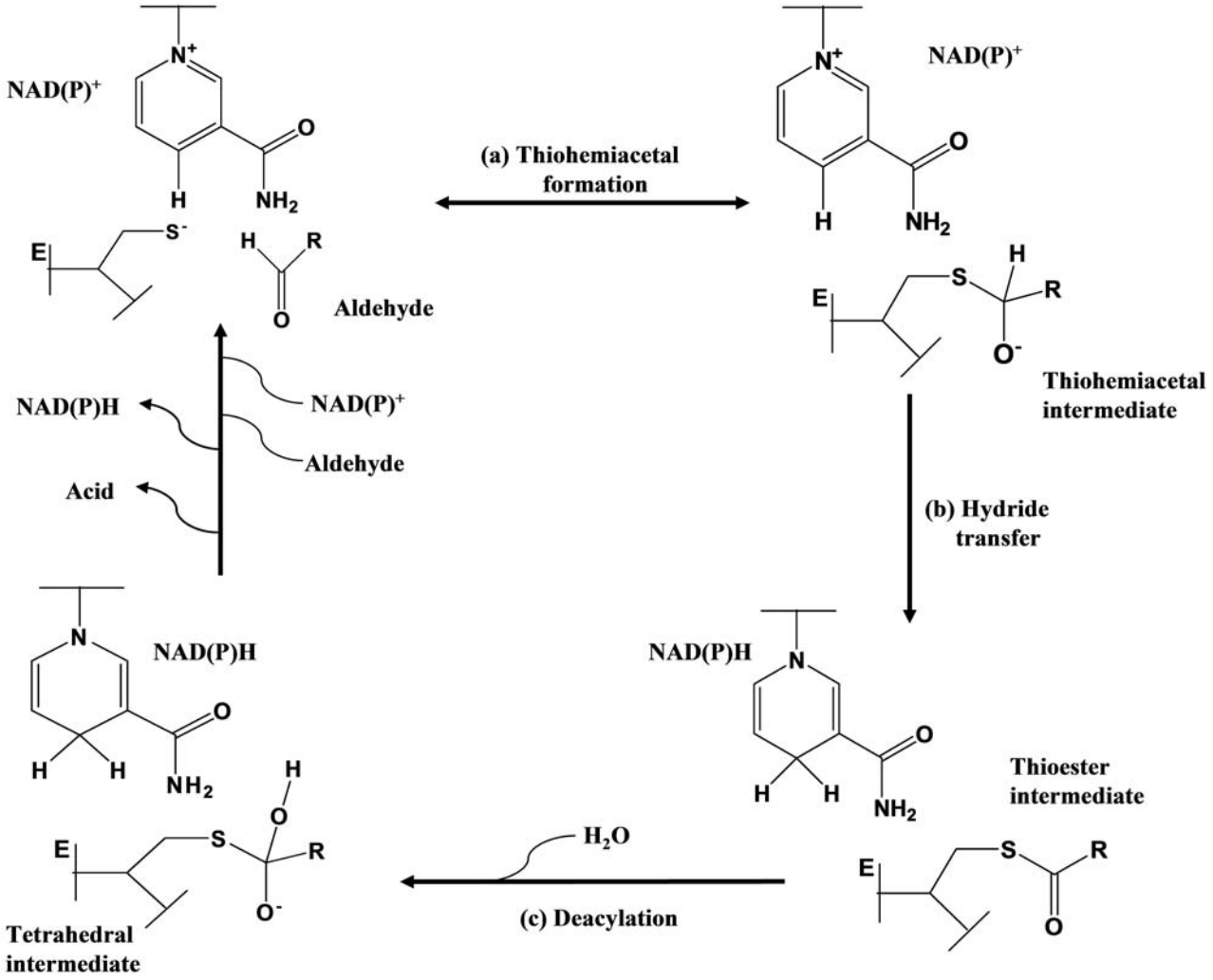

Fig. 1. Proposed catalytic mechanism of the dehydrogenase reaction.

[17], *Ovis aries* ALDH1 (*Oa*ALDH1) [18], *Mus musculus* ALDH (*Mm*ALDH) [19], *Streptococcus mutans* ALDH (*Sm*ALDH) [20], and *Pseudomonas aeruginosa* betaine aldehyde dehydrogenase (*Pa*BADH) [21]. Structural and other evidence reveals that the catalytic mechanism of the ALDH family involves acylation and deacylation steps (Fig. 1). In the acylation step the active site cysteine sulfur makes a nucleophilic attack on the carbonyl carbon of the aldehyde. Then the hydrogen leaves as a hydride and attacks $NAD(P)^+$ to yield NAD(P)H. The enzyme active site then undergoes a rearrangement wherein the NAD(P)H molecule is moved, creating space for a water molecule to access the substrate. In the deacylation step, the nucleophilic water molecule at glutamate in the active site and attacks the carbonyl carbon to generate sulfhydryl as a leaving group.

Bacillus licheniformis is a Gram-positive, spore-forming soil bacterium that is closely related to the well-studied model organism *Bacillus subtilis* [22, 23]. This species produces an assortment of extracellular enzymes that may contribute to nutrient cycling in nature. Commercially, *B. licheniformis* is employed extensively for the production of exoenzymes [24] as well as smaller compounds like the antibiotic bacitracin [25, 26] and various organic metabolites [27, 28]. More than 10 *ALDH* genes have been identified in this bacterium [29], and one of these genes, *ybcD*, encodes an ALDH enzyme consisting of 488 amino acid residues. Very recently, the *ybcD* gene has been cloned and overexpressed in *Escherichia coli* [30]. The recombinant enzyme prefers NAD^+ as a cofactor in the oxidation of aliphatic aldehydes.

To understand the structure–function relationship of the cloned *B. licheniformis* ALDH (*Bl*ALDH) [30], a directed evolution strategy was pursued in this study to elucidate the role of the conserved Glu255 and Cys289 residues. The data presented herein indicate that these two residues are important for the dehydrogenase activity of the enzyme.

MATERIALS AND METHODS

Materials, bacterial strains, and growth conditions. Luria–Bertani (LB) medium was purchased from Difco Laboratories (USA). The oligonucleotides used in site-directed mutagenesis were synthesized by Mission Biotechnology Inc. (Taiwan). Ni^{2+}-nitrilotriacetate (Ni^{2+}-NTA) resin was acquired from Qiagen Inc. (USA). Protein assay reagents, acrylamide, bis-acrylamide, TEMED, and ammonium persulfate were from Bio-Rad Laboratories (USA). NAD^+, NADH, propionaldehyde, and guanidine hydrochloride (GdnHCl) were from Sigma-Aldrich (USA). Unless indicated otherwise, all other chemicals were commercial products of analytical or molecular biological grade.

Escherichia coli NovaBlue (Novagen Inc., USA) was used in the preparation of plasmids, and *E. coli* XL-1 Blue (Stratagene, USA) was used for site-directed mutagenesis.

T5 RNA-polymerase-mediated gene expression was performed in *E. coli* M15 (pRep4) (Qiagen). *Escherichia coli* strains were grown aerobically with shaking in LB medium at 37°C. As required, ampicillin and kanamycin were supplemented to a final concentration of 100 and 25 μg/ml, respectively.

Computer modeling. Construction of molecular models, structure optimization, and conformational analysis were carried out with Discovery Studio 1.7 (Accelrys Inc., USA) using the CHARMM empirical force field [31]. The structure of *Bl*ALDH was simulated using *Pa*BADH structure (PDB code: 2wme) as the template. The energy minimization of the model was iterated 500 cycles by the steepest descent method and finally convergence at 0.002 kcal/mol Å.

Site-directed mutagenesis. Mutations were introduced into pQE-*ybcD* plasmid [30] using the QuikChange™ XL site-directed mutagenesis kit (Stratagene) according to the manufacturer's protocol. Two overlapping complementary primers containing the desired nucleotide changes were designated for each mutation (table). The mutagenic PCR reaction mixture consisted of 20 mM Tris-HCl (pH 8.8), 10 mM KCl, 10 mM $(NH_4)_2SO_4$, 2 mM $MgSO_4$, 0.1% Triton X-100, 0.1 mg/ml nuclease-free bovine serum albumin (BSA), 12 ng of template DNA, 0.5 mM dNTPs, 1 μM each of the complementary primers, and 3.6 units of *Pfu* DNA polymerase. Mutant DNA was generated with a thermal cycling program of 2 min at 95°C and 16 cycles of 30 sec at 95°C, 60 sec at 55°C, and 12 min at 68°C on an Applied Biosystems (USA) thermal cycler. The amplified products were digested with 10 units of *Dpn*I at 37°C for 1 h prior to their use for transformation into *E. coli* XL-1 blue cells. Mutations were confirmed by DNA sequencing with a dye terminator cycle sequencing kit and an automatic DNA sequencer (Applied Biosystems).

Expression and purification of the parental and mutant enzymes. To express the parental and mutant *Bl*ALDHs, *E. coli* M15 cells harboring pQE-*ybcD* or each of the mutated plasmids were cultivated in 100 ml of LB media containing 100 μg/ml ampicillin and 25 μg/ml kanamycin to A_{600} of 0.5 and then induced with 50 μM isopropyl β-D-thiogalactopyranoside (IPTG). After an additional incubation at 37°C for 12 h, the cells were collected by centrifugation and resuspended in 3 ml of binding buffer (5 mM imidazole, 0.5 M NaCl, and 50 mM NaH_2PO_4, pH 7.9). The resuspended cells were cooled on ice and disrupted by sonication (30-sec bursts and pauses for 5 min). The resulting extracts were clarified by centrifugation at 12,000*g* for 20 min to remove cell debris, and the supernatants were subsequently mixed with Ni^{2+}-NTA resin pre-equilibrated with the binding buffer. After extensive washing with the binding buffer, the His_6-tagged proteins were eluted from the resin by buffer containing 0.5 M imidazole, 0.5 M NaCl, and 50 mM NaH_2PO_4 (pH 7.9).

Gel electrophoresis and determination of protein concentration. SDS-PAGE was performed with a Bio-Rad Protean III Dual Slab Cell (Bio-Rad) using a discontinuous buffer system [32]. The protein samples were suspended in SDS-PAGE loading buffer (5% 2-mercaptoethanol, 2% SDS, 0.1% bromophenol blue, and 10% glycerol in 50 mM Tris-HCl buffer, pH 6.8) and applied to 12% separating gel. After electrophoresis, the gels were

Oligonucleotide primers used for site-directed mutagenesis

Protein	Nucleotide sequence (5′→3′)*	Codon change
E255D	GCGAAGTACCAGCTTGACATGGGCGGCAAA	GAG → GAC
E255K	GCGAAGTACCAGCTTAAGATGGGCGGCAAA	GAG → AAG
C289R	TCGACAGGCCAAAAGCGTACAGCGACAAGC	TGT → CGT
C289P	TCGACAGGCCAAAAGTTTACAGCGACAAGC	TGT → TTT
C289D	TCGACAGGCCAAAAGGATACAGCGACAAGC	TGT → GAT

* Only sense sequences are shown and mismatches with the original sequence of the *ybcD* gene are underlined.

stained with 0.25% Coomassie brilliant blue dissolved in 50% methanol/10% acetic acid and then destained in a solution of 30% methanol/10% acetic acid. The protein size markers were phosphorylase *b* (97.4 kDa), BSA (66.3 kDa), ovalbumin (45.0 kDa), carbonic anhydrase (31.0 kDa), trypsin inhibitor (21.5 kDa), and hen egg lysozyme (14.4 kDa).

Protein concentrations were determined by the Coomassie G dye binding technique of Bradford [33] using BSA as the standard.

Enzymatic assay. *Bl*ALDH activity was assayed according to the method previously described [34]. The assay mixture contained 50 mM sodium phosphate buffer (pH 7.0), 1 mM dithiothreitol, and the enzyme solution at a suitable dilution. The reaction was initiated by addition of 2 mM propionaldehyde and 4 mM NAD^+ into the reaction mixture. After incubation at 37°C for 10 min, the reaction was terminated by heating at 80°C for 5 min. Enzymatic activity was calculated from the reduction of NAD^+ to NADH at 340 nm, using the NADH extinction coefficient of 6.22 $mM^{-1}\cdot cm^{-1}$. One unit of *Bl*ALDH activity was defined as the amount of enzyme that reduced 1 μmol of NAD^+ to NADH per minute.

Circular dichroism (CD) spectroscopy. CD spectra in the far UV-region (190-240 nm) were recorded on a JASCO model J-815 equipped with a Peltier thermostatted cuvette holder under constant nitrogen flow. The photomultiplier voltage was always below 600 V in the analyzed region. Each scanning was repeated 10 times and the average was reported. Data were corrected for the buffer effect, and the experimental results were expressed as molar ellipticity [θ] in units of $deg\cdot cm^2\cdot dmol^{-1}$ according to Eq. (1):

$$[\theta] = \frac{\theta}{10 \cdot C \cdot l}, \quad (1)$$

where l represents the light path length (cm), C is the molar concentration of protein, and θ denotes the observed ellipticity (mdeg).

The unfolding transition curves for the parental and mutant *Bl*ALDHs were obtained by monitoring the ellipticity at 222 nm in a 1-mm cell. The temperature was increased with a heating rate of 4°C/min from 20 to 100°C and the transition midpoint (T_m) was recorded.

Fluorescence spectroscopy. Fluorescence spectra of the recombinant enzymes were monitored at 30°C in a JASCO FP-6500 fluorescence spectrophotometer with excitation wavelength of 280 nm. All spectra were corrected for buffer absorption. The fluorescence emission spectra of protein samples were recorded from 300 to 400 nm at a scanning speed of 240 nm/min. The maximal peak of the fluorescence spectrum and the change in fluorescence intensity were used in monitoring the unfolding processes of the enzyme. Both the red shift and the change in fluorescence intensity were analyzed together using the average emission wavelength (AEW) (λ) according to Eq. (2) [35]:

$$\langle\lambda\rangle = \frac{\sum_{i=\lambda_1}^{\lambda_N}(F_i \cdot \lambda_i)}{\sum_{i=\lambda_1}^{\lambda_N} F_i}, \quad (2)$$

where F_i is the fluorescence intensity at the specific emission wavelength (λ_i).

Unfolding of recombinant enzymes by GdnHCl. The unfolding experiments of parental and mutant enzymes were examined in different concentrations of GdnHCl in 50 mM sodium phosphate buffer (pH 7.0) at room temperature. The preliminary experiments showed that 30-min incubation time was sufficient for the unfolding to achieve equilibrium at all denaturant concentrations.

Unfolding curves of the parental and mutant enzymes were used to calculate the thermodynamic parameters by global fitting of the experimental data. The two-state unfolding model (Scheme) was described by Eq. (3) [36]:

$$N \underset{}{\overset{K_{N\text{-}U}}{\longleftrightarrow}} U$$

Scheme

$$y_{obs} = \frac{(y_N + m_f[D]) + (y_U + m_u[D]) \cdot \exp[-(\Delta G_{H_2O} - m[D])/RT]}{1 + \exp[-(\Delta G_{H_2O} - m[D])/RT]}, \quad (3)$$

where y_{obs} is the observed biophysical signal, y_N and y_U are the intercepts, m_f and m_u are the slopes of the pre- and post-transition baselines, T is temperature, R is the universal gas constant, [D] is the concentration of GdnHCl, ΔG_{H_2O} represents an estimate of the conformational stability of the protein in the absence of denaturant, and m is a measure of the dependence of ΔG.

RESULTS AND DISCUSSION

Sequence comparison and homology modeling. Using the CLUSTALW program from ExPASy Proteomics server (http://tw.expasy.org), we observed that *Bl*ALDH sequence shares 40, 40, 38, 36, 35, and 20% identity with the primary sequence of *Pa*BADH (Swiss-Prot Q9HTJ1), *Oa*ALDH1 (Swiss-Prot P51977), *Bs*ALDH2 (Swiss-Prot P20000), *Gc*ALDH9 (Swiss-Prot P56533), *Sm*ALDH (Swiss-Prot Q59931), and *Rn*ALDH (Swiss-Prot P11883), respectively. Although the sequence identities for the different ALDHs can be as low as 20%, the structures determined so far adopt the same basic fold with one dinucleotide-binding domain, one catalytic domain, and one oligomerization domain [15-20]. Unlike the classical

Rossmann fold, the nucleotide-binding domain of ALDHs consists of only five parallel β-strands. The interaction between the pyrophosphate moiety of the nucleotide and the enzyme occurs via the loop between strand β_1 and helix α_8. This arrangement results in a significantly different conformation of the co-substrate compared to proteins with the Rossmann fold. The catalytic domain adopts an α/β fold and contains the conserved active site cysteine (Cys286 in *Pa*BADH, Cys303 in *Oa*ALDH1, Cys322 in *Bs*ALDH2, Cys297 in *Gc*ALDH9, Cys284 in *Sm*ALDH, and Cys244 in *Ra*ALDH). Despite many biochemical and mutagenesis studies, the mechanism and the role of putatively essential residues of this reaction remain to be elucidated at the molecular level [37], especially the invariant glutamate 268 (numbering according to *Bs*ALDH2). This glutamate residue has been implied to function as a general base for the deprotonation of the active site cysteine in *Bs*ALDH2 [16]. The corresponding residue seems to be involved only in co-substrate binding in *Rn*ALDH3 [15]. However, in the case of *Sm*ALDH it has been suggested to play an essential role in deacylation by activating a water molecule that hydrolyzes the intermediate [38].

In the lack of crystal structures, homology modeling has been shown to be a valuable tool for gaining insight into the active site pocket of a number of enzymes [39-41]. As mentioned above, *Bl*ALDH has highest sequence identity with *Pa*BADH, and this fact guarantees a reliable building of homology structure. Given that the conserved Cys303 and Glu268 residues (numbering is for *Bs*ALDH2) are necessary for the catalytic mechanism of ALDHs, the location of the corresponding Glu255 and Cys289 residues in the putative active site of *Bl*ALDH warranted their exploration as the essential residues for the enzyme (Fig. 2; see color insert).

Purification and characterization of parental and mutant enzymes. Due to the potential importance of the conserved Glu255 and Cys289, these two residues were selected for site-directed mutagenesis. After verification of the altered sequences, pQE-*Bl*ALDH and each of the mutated plasmids were transformed into *E. coli* M15 (Prep4) for IPTG-induced gene expression. The overexpression of parental and mutant enzymes was assessed by analyzing protein profiles of the whole cell lysate preparations, where all these proteins were expressed as a predominant band with an estimated molecular mass of 53 kDa (data not shown). The parental and mutant enzymes in the crude extracts were further purified to near homogeneity by Ni^{2+}-NTA resin (Fig. 3a). The purification procedure resulted in a yield of 25-34% of the ALDH activity for the recombinant enzymes.

The assay of enzymatic activity with 2 mM propionaldehyde showed that the purified *Bl*ALDH had a specific activity of 8.3 ± 0.2 U/mg protein (Fig. 3b). Substitution of Glu255 with either Asp or Lys resulted in mutant enzyme with diminished activity. Similarly, the ALDH activity was nearly abolished in C289P, C289R, and C289D mutant enzymes. These results indicate that residues Glu255 and Cys289 play an important role in the functionality of *Bl*ALDH.

Structural analysis of parental and mutant enzymes. To determine whether the differences in catalytic activity between the mutant enzymes and the parental *Bl*ALDH were due to major structural changes of the variants, we recorded their far-UV CD and tryptophan fluorescence spectra (Fig. 4). The parental enzyme has two ellipticity minima of almost equal amplitude at 208 and 218 nm, whereas the negative ellipticity of E255K at 208 nm was slightly more pronounced that at 218 nm (Fig. 4a). In general, the CD spectra of the mutant enzymes were similar to that of the parental *Bl*ALDH. The intrinsic tryptophan fluorescence spectrum of the parental *Bl*ALDH was characterized by a peak centered at 336.1 nm (Fig. 4b). Most of the mutant enzymes had tryptophan fluorescence

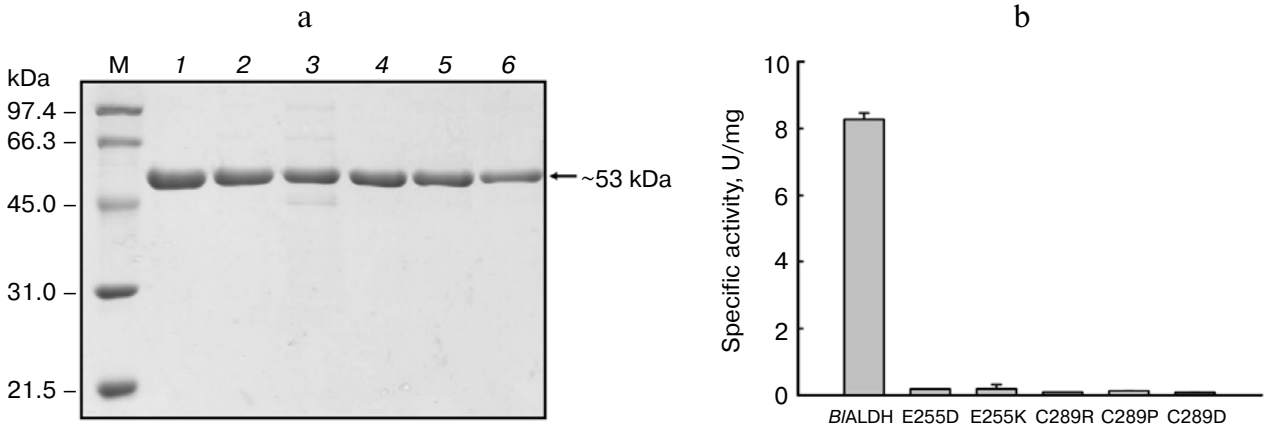

Fig. 3. SDS-PAGE analysis (a) and specific activity (b) of parental and mutant enzymes. Lanes: M, protein size markers; *1*) BlALDH; *2*) E255D; *3*) E255K; *4*) C289R; *5*) C289P; *6*) C289D.

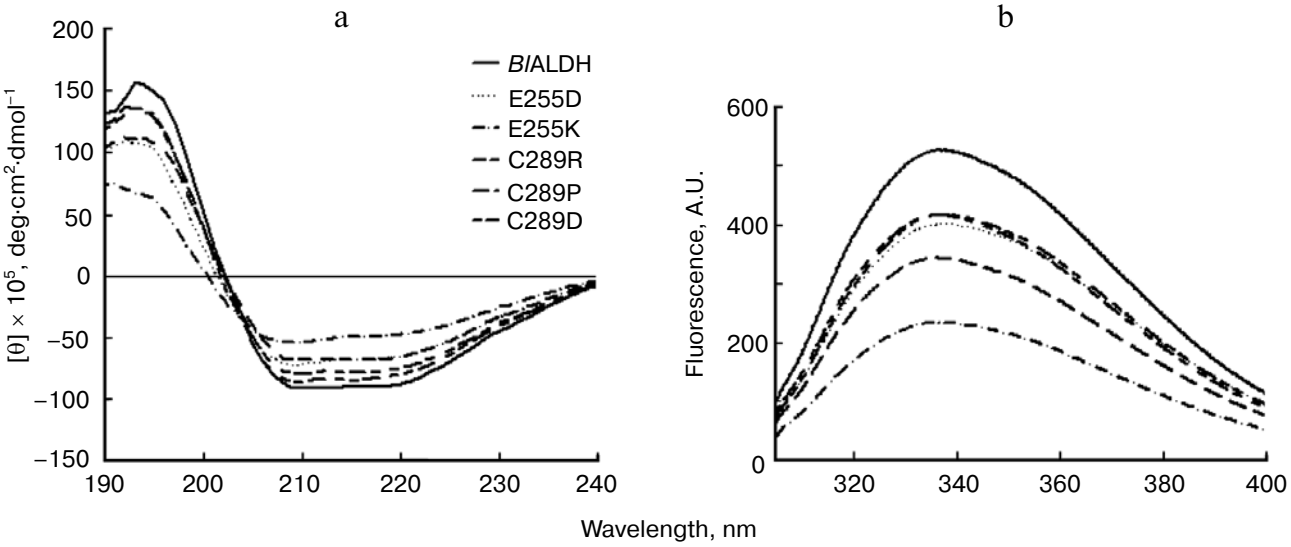

Fig. 4. Far-UV CD (a) and intrinsic tryptophan fluorescence (b) spectra of parental and mutant enzymes. An average of 10 spectra of each protein was recorded. The protein concentration was approximately 0.25 mg/ml.

spectra similar to that of the parental *Bl*ALDH, with the exception of E255D in which the spectrum slightly shifted to the red with a peak centered at 338 nm. The relative fluorescence intensity of the mutant enzymes also varied appreciably from that of the parental *Bl*ALDH. The intensity of E255D, E255K, C289R, C289P, and C289D was decreased 21-57% with respect to the parental enzyme. These observations suggest that minor changes in the protein structure have been occurred as a consequence of E255 and C289 mutations.

To probe the structural integrity of the parental and mutant enzymes, their thermal denaturation patterns were determined by following the changes in ellipticity at 222 nm (Fig. 5). The denaturation curves of the parental and mutant enzymes showed single sigmoidal transitions. Midpoints of thermal transition, T_m, were calculated to be 51, 45, 55, 56, 50 and 54°C for parental *Bl*ALDH, E255D, E255K, C289R, C289P, and C289D, respectively. The T_m of E255D was 6°C lower than the parental T_m. However, substitution of this residue with lysine induced an obvious effect on the thermal stability. The T_m value for C289R and C289D was also higher than that of the parental *Bl*ALDH. These data clearly indicate that E255 and C289 mutations have a significant effect on the thermal stability of the enzyme.

Unfolding of parental and mutant enzymes by GdnHCl. The function of a protein depends on its ability to acquire a unique three-dimensional structure [43]. GdnHCl is commonly used as a protein denaturant, which generally brings about unfolding of proteins by disrupting their secondary and tertiary structures. *Bl*ALDH contains five tryptophanyl residues (Fig. 2a). Thus, the GdnHCl-induced unfolding is very suitable for conformational stability studies of this enzyme. Unfolding of the parental and mutant enzymes at different concentrations of GdnHCl was therefore performed, and the data are shown in Fig. 6. The AEW that reports on the changes in both fluorescence wavelength and fluorescence intensity was used to calculate the thermodynamic parameters of the unfolding process. As shown in Fig. 6a, *Bl*ALDH started to unfold at a very low concentration of denaturant with $[GdnHCl]_{0.5,N\text{-}U}$ of 0.92 M. By fitting Eq. (3), the calculated free energy change (ΔG_{H_2O}) for the N ↔ U process was 2.98 kcal/mol. The fluorescence signals of

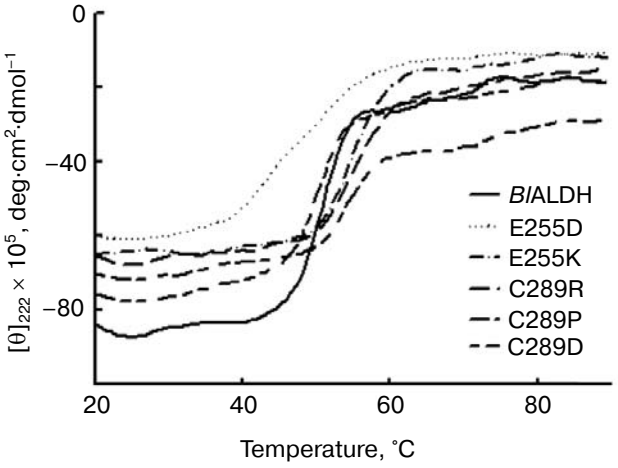

Fig. 5. Thermal denaturation of parental and mutant enzymes dissolved in 50 mM sodium phosphate buffer (pH 7.0) as monitored by CD signal at 222 nm. The protein concentration was approximately 0.25 mg/ml.

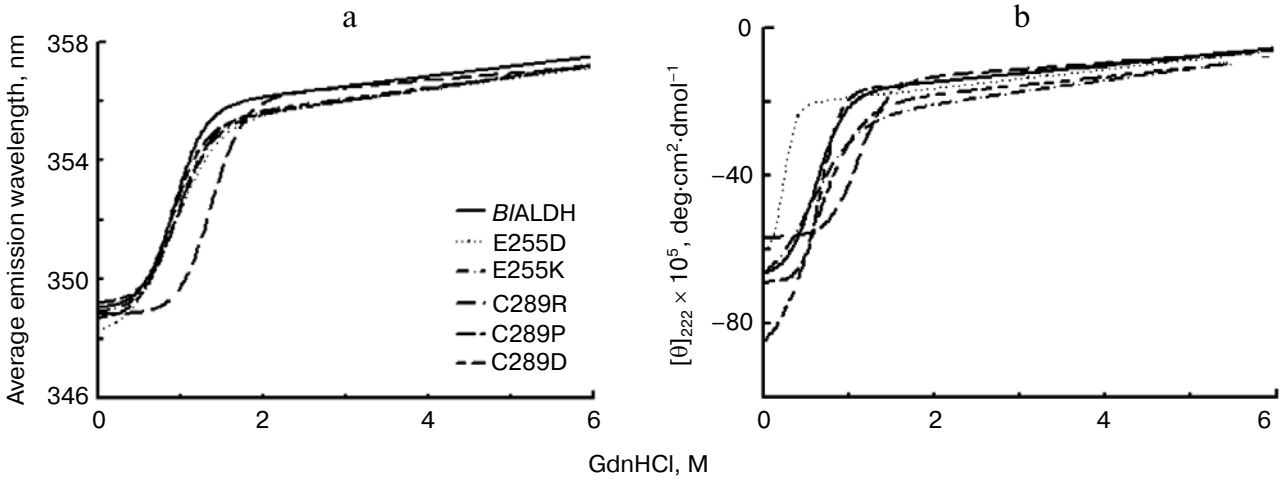

Fig. 6. GdnHCl-induced denaturation of parental and mutant enzymes. a) Changes in intrinsic tryptophan fluorescence as a function of GdnHCl concentration. Data are represented as the AEW, taking the value observed for native protein in the absence of denaturant as the control. b) Changes in CD signal at 222 nm as a function of GdnHCl concentration. The smooth curves are computer-generated best-fit lines according to a two-state unfolding model (Eq. (3)).

GdnHCl-induced E255D, E255K, C289R, C289P, and C289D were also monophasic processes, which showed $[GdnHCl]_{0.5,N\text{-}U}$ of 0.91, 0.95, 1.37, 0.97, and 0.96 M, corresponding to ΔG_{H_2O} of 2.05, 2.71, 4.29, 2.92, and 2.80 kcal/mol, respectively, for the N ↔ U process. Similar results were observed with CD spectra (Fig. 6b). *Bl*ALDH, E255D, E255K, C289R, C289P, and C289D showed $[GdnHCl]_{0.5,N\text{-}U}$ of 0.60, 0.22, 0.52, 1.10, 0.57, and 0.67 M, corresponding to free energy change of 2.14, 2.01, 1.18, 3.84, 1.41, and 3.70 kcal/mol, respectively, for the N ↔ U process. Based on these observations, it can be concluded that a lower concentration of GdnHCl was required to start the unfolding of *Bl*ALDH. This allows one to distinguish the conformation stabilities between the parental and mutant enzymes and reflects that the protein structure of *Bl*ALDH has been changed as a consequence of mutations.

Influence of mutations on the reaction mechanism. The reaction mechanism of ALDHs involves three main steps (Fig. 1) [44]: (i) nucleophilic attack of the catalytic cysteine (Cys302 in *Bs*ALDH2) on the carbonyl carbon of the aldehyde, which forms a tetrahedral hemithioacetal intermediate covalently bound to the enzyme; (ii) hydride transfer from the tetrahedral hemithioacetal to the pyridine ring of $NAD(P)^+$, which produces a thioester intermediate; and (iii) nucleophilic attack of a water molecule on the thioester, which generates a second tetrahedral intermediate and results in the release of the acid product. It is well accepted that Glu268 (numbering according to *Bs*ALDH2) is the general base in the activation of the hydrolytic water molecule [38, 45, 46]. In fact, residues Cys302 and Glu268 corresponding to Cys289 and Glu255 of *Bl*ALDH are strictly conserved among the ALDH proteins with dehydrogenase activity.

Crystal structures of several ALDHs from different organisms have been determined in the absence and presence of $NAD(P)^+$, NAD(P)H, aldehydes, or acid products, and the residues involved in each step of the catalytic mechanism have been elucidated at the atomic level. It was soon realized that the ALDH proteins do not undergo major conformational changes upon the binding of the cofactors [16], but that there is a conformational flexibility in the catalytic Cys302 [20, 47-49] and Glu268 residues [21, 48-51]. Cys302 has been proposed to adopt two different conformations: one, located far away from the carbonyl carbon of the bound aldehyde, is called the resting conformation [21, 37, 47-50], and the other one, situated close to this carbon in the correct position to perform the nucleophilic attack, is called attacking conformation [16, 37, 48-50, 52]. Glu268 has been observed to adopt three stable conformations: inside, intermediate, and outside. The inside conformation is sterically incompatible with the bound oxidized cofactor, and it has been proposed that Glu268 in this conformation can activate Cys302 for the nucleophilic attack because the carbonyl group is close to the thiol [37, 48-50, 53]. The intermediate conformation is sterically compatible with the oxidized cofactor and is thought to the one suited for the activation of the hydrolytic water molecule [15, 48-50, 54-56]. In the outside conformation, Glu268 releases the proton that was previously taken from either the catalytic Cys or the hydrolytic water molecule through a proton relay mechanism [21].

As shown in Fig. 7 (see color insert), two conformations for Cys289 and three conformations for Glu255 can be observed in the modeled active site of *Bl*ALDH. Given that Cys302 is the catalytic residue, and that the conformational flexibility of Glu268 plays an important role in

the deacylation step of the ALDH-catalyzed reaction, the corresponding Glu255 and Cys289 residues of *Bl*ALDH might play similar roles to those of other ALDH enzymes.

In summary, sequence alignment showed that residues Glu255 and Cys289 of *Bl*ALDH are conserved in the ALDH family. Computer modeling and site-directed mutagenesis results provided definitive evidence that Glu255 and Cys289 are critical for the function of *Bl*ALDH. Glutamate 255 may function as a general base necessary for the initial activation of cysteine 289. The conservation of these two residues suggests that their roles can be extended to the entire ALDH family.

The authors are very grateful to the National Science Council of Taiwan for the financial supports (NSC 95-2313-B-415-012-MY3 and NSC 95-2313-B-415-001).

REFERENCES

1. Perozich, J., Nicholas, H., Wang, B. C., Lindahl, R., and Hempel, J. (1999) *Protein Sci.*, **8**, 137-146.
2. Vasiliou, V., Pappa, A., and Petersen, D. (2000) *Chem. Biol. Interact.*, **129**, 1-19.
3. Sripo, T., Phongdara, A., Wanapu, C., and Caplan, A. B. (2002) *Appl. Environ. Microbiol.*, **62**, 171-179.
4. Chang, C., and Yoshida, A. (1994) *Gene*, **148**, 331-336.
5. Fontaine, L., Meynial-Salles, I., Girbal, L., Yang, X., Croux, C., and Soucaille, P. (2002) *J. Bacteriol.*, **184**, 821-830.
6. Pappa, A., Estey, T., Manzer, R., Brown, D., and Vasiliou, V. (2003) *Biochem. J.*, **376**, 615-623.
7. Grochowski, L. L., Xu, H., and White, R. H. (2006) *J. Bacteriol.*, **188**, 2836-2844.
8. Bains, J., and Boulanger, M. J. (2008) *J. Mol. Biol.*, **379**, 597-608.
9. Cao, Y., Liao, L., Xu, X. W., Oren, A., and Wu, M. (2008) *Extremophiles*, **12**, 849-854.
10. Jo, J. E., Mohan Raj, S., Rathnasingh, C., Selvakumar, E., Jung, W. C., and Park, S. (2008) *Appl. Microbiol. Biotechnol.*, **81**, 51-60.
11. Stiti, N., Adewale, I. O., Petersen, J., Bartels, D., and Kirch, H. H. (2011) *Biochem. J.*, **434**, 459-471.
12. Sophos, N. A., and Vasiliou, V. (2003) *Chem. Biol. Interact.*, **143/144**, 5-22.
13. Vasiliou, V., and Nebert, D. W. (2005) *Hum. Genom.*, **2**, 138-143.
14. Kavanagh, K. L., Jornvall, H., Persson, B., and Oppermann, U. (2008) *Cell. Mol. Life Sci.*, **65**, 3895-3906.
15. Liu, Z. J., Sun, Y. J., Rose, J., Chung, Y. J., Hsiao, C. D., Chang, W. R., Kuo, I., Perozich, J., Lindahl, R., Hempel, J., and Wang, B. C. (1997) *Nat. Struct. Biol.*, **4**, 317-326.
16. Steinmetz, C. G., Xie, P., Weiner, H., and Hurley, T. D. (1997) *Structure*, **5**, 701-711.
17. Johansson, K., el Almad, M., Ramaswamy, S., Hjelmqvist, L., Jornvall, H., and Eklund, H. (1998) *Protein Sci.*, **7**, 2106-2117.
18. Moore, S. A., Baker, H. M., Blythe, T. J., Kitson, K. E., Kitson, T. M., and Baker, N. (1998) *Structure*, **6**, 1541-1551.
19. Lamb, A. L., and Newcomer, M. E. (1999) *Biochemistry*, **38**, 6003-6011.
20. Cobessi, D., Tete-Favier, F., Marchal, S., Branlant, G., and Aubry, A. (1999) *J. Mol. Biol.*, **290**, 161-173.
21. Gonzalez-Segura, L., Rudino-Pinera, E., Munoz-Clares, R. A., and Horjales, E. (2009) *J. Mol. Biol.*, **385**, 542-557.
22. O'Donnell, A. G., Norris, J. R., Berkeley, R. C. W., Claus, D., Kaneko, T., Logan, N. A., and Nozaki, R. (1980) *Int. J. Syst. Bacteriol.*, **30**, 448-459.
23. Xu, D., and Cote, J. C. (2003) *Int. J. Syst. Evol. Microbiol.*, **53**, 695-704.
24. Schallmey, M., Singh, A., and Ward, O. P. (2004) *Can. J. Microbiol.*, **50**, 1-17.
25. Ming, L. J., and Epperson, D. J. (2002) *J. Inorg. Biochem.*, **91**, 48-58.
26. Murphy, T., Roy, I., Harrop, A., Dixon, K., and Keshavarz, T. (2007) *J. Biotechnol.*, **131**, 397-403.
27. Birrer, G. A., Cromwick, A. M., and Gross, R. A. (1994) *Int. J. Biol. Macromol.*, **16**, 265-275.
28. Zuo, R. (2007) *Appl. Microbiol. Biotechnol.*, **76**, 1245-1253.
29. Veith, B., Herzberg, C., Steckel, S., Feesche, J., Maurer, K. H., Ehrenreich, P., Baeumer, S., Henne, A., Liesegang, H., Merkl, R., Ehrenreich, A., and Gottschalk, G. (2004) *J. Mol. Microbiol. Biotechnol.*, **7**, 204-211.
30. Lo, H. F., and Chen, Y. J. (2010) *Mol. Biotechnol.*, **46**, 157-167.
31. Nimlos, M. R., Matthews, J. F., Crowley, M. F., Walker, R. C., Chukkapalli, G., Brady, J. W., Adney, W. S., Cleary, J. M., Zhong, L., and Himmel, M. E. (2007) *Protein Eng. Des. Sel.*, **20**, 179-187.
32. Laemmli, U. K. (1970) *Nature*, **227**, 680-685.
33. Bradford, M. M. (1976) *Anal. Biochem.*, **72**, 248-254.
34. Leal, N. A., Havemann, G. D., and Bobik, T. A. (2003) *Arch. Microbiol.*, **180**, 353-361.
35. Royer, C. A., Mann, C. J., and Mathews, C. R. (1995) *Protein Sci.*, **2**, 1844-1852.
36. Pace, C. N. (1990) *Trends Biotechnol.*, **8**, 93-98.
37. Cobessi, D., Tete-Favier, F., Marchal, S., Branlant, G., and Aubry, A. (2000) *J. Mol. Biol.*, **300**, 141-152.
38. Marchal, S., Rahuel-Clermont, S., and Branlant, G. (2000) *Biochemistry*, **39**, 3327-3335.
39. Li, N., Ma, D. L., Liu, X., Wu, L., Chu, X., Wong, K. Y., and Li, D. (2007) *Protein J.*, **26**, 569-576.
40. Zhao, L., Liu, D., Zhang, Q., Zhang, S., Wan, J., and Xiao, W. (2008) *FEMS Microbiol. Lett.*, **277**, 37-43.
41. Lo, H. F., Chen, H. L., Yen, S. Y., Ong, P. L., Chang, W. S., and Chang, C. T. (2010) *Biologia*, **65**, 399-407.
42. DeLano, W. L. (2002) *The PyMOL Molecular Graphics System*, DeLano Scientific, Palo Alto, CA, USA, http://www.pymol.org/
43. Thornton, J. M., Orengo, C. A., Todd, A. E., and Pearl, F. M. (1999) *J. Mol. Biol.*, **293**, 333-342.
44. Feldman, R. I., and Weiner, H. (1972) *J. Biol. Chem.*, **247**, 267-272.
45. Wang, X., and Weiner, H. (1995) *Biochemistry*, **34**, 237-243.
46. Vedadi, M., Szittner, R., Smillie, L., and Meighen, E. (1995) *Biochemistry*, **34**, 16725-16732.
47. Ahvazi, B., Coulombe, R., Delarge M., Vedadi, M., Zhang, L., Meihgen, E., and Vrielink, A. (2000) *Biochem. J.*, **349**, 853-861.

48. Gruez, A., Roig-Zamboni, V., Grisel, S., Salomoni, A., Valencia, C., Campanacci, V., Tegoni, M., and Cambillau, C. (2004) *J. Mol. Biol.*, **343**, 29-41.
49. Inagaki, E., Ohshima, H., Takahashi, C., Yokoyama, S., and Tahirov, T. H. (2006) *J. Mol. Biol.*, **362**, 490-501.
50. Tsybovsky, Y., Donato, H., Krupenko, N. I., Davies, C., and Krupenko, S. A. (2007) *Biochemistry*, **46**, 2917-2929.
51. Tylichova, M., Kopecny, D., Morera, S., Briozzo, P., Lenobel, R., Snegaroff, J., and Sebela, M. (2010) *J. Mol. Biol.*, **396**, 870-882.
52. Di Constanzo, L., Gomez, G. A., and Christiaanson, D. W. (2007) *J. Mol. Biol.*, **366**, 481-493.
53. Perez-Miller, S. J., and Hurley, T. D. (2003) *Biochemistry*, **42**, 7100-7109.
54. Larson, H. N., Zhou, J., Chen, Z., Stamler, J. S., Weiner, H., and Hurley, T. D. (2007) *J. Biol. Chem.*, **282**, 12940-12950.
55. Pohl, E., Brunner, N., Wilmanns, M., and Hensel, R. (2002) *J. Biol. Chem.*, **277**, 19938-19945.
56. Lorentzen, E., Hensel, R., Knura, T., Ahmed, H., and Pohl, E. (2004) *J. Mol. Biol.*, **341**, 815-828.